

# Modeling of Magnetisation and Intrinsic Properties of Ideal Type-II Superconductor in External Magnetic Field

Oleg A. Chevtchenko<sup>\*1</sup>, Johan J. Smit<sup>1</sup>, D.J. de Vries<sup>2</sup>, F.W.A. de Pont<sup>2</sup>

<sup>1</sup>Technical University of Delft, The Netherlands

<sup>2</sup>Comsol BV Rontgenlaan 37, 2719 DX Zoetermeer, The Netherlands

\*Corresponding author: EWI, TU Delft, Postbus 5031, 2600 GA Delft, NL; [o.chevtchenko@tudelft.nl](mailto:o.chevtchenko@tudelft.nl)

**Abstract:** In this paper, a COMSOL model is developed for type-II superconductors with Ginzburg-Landau (GL) parameter  $\kappa = 50$ : a typical value for modern high field-, high current superconductors.

As a first step, the two-dimensional time-dependent GL equations for low  $\kappa$ -values are implemented in COMSOL using an approach similar to that of Alstrøm et al<sup>1</sup>. While it doesn't take much computational effort to reproduce results at  $\kappa = 2$ , the situation becomes more challenging at  $\kappa = 50$  ( $\kappa = \lambda/\xi$ , with  $\lambda$  being related to the geometry size and  $\xi$  related to the mesh size).

In order to overcome the complication, periodicity has been used: a periodic hexagonal unit cell of variable size is introduced, always containing a single flux quantum  $\Phi_0$  (resulting in an ideal periodic Flux-Line Lattice, FLL, that is, an Abrikosov lattice). From this, magnetisation curves are computed and compared to those of Brandt. Excellent agreement is found over the whole range of external magnetic field values.

Additionally, fundamental properties such as the value of the upper critical field and the structure of a vortex are reproduced and compared to analytical predictions. Excellent agreement is found on all these points, validating this model as a candidate for further research on pinning effects in type-II superconductors at  $\kappa = 2$  to 50.

**Keywords:** Type-II superconductor, Ginzburg-Landau equations, vortex, flux line lattice, magnetic field, magnetisation.

## 1. Introduction

The two dimensional, time dependent Ginzburg-Landau (GL) equations for vortex dynamics in ideal type-II superconductors were solved using COMSOL with the approach of Alstrøm<sup>1</sup>. Using COMSOL's built-in PDE interfaces, coupled magnetic vector potential  $A$  and order parameter  $\psi$  fields were solved on a two dimensional finite domain subjected to external perpendicular magnetic field.

After reproducing the results on vortex dynamics from [1] for GL parameter  $\kappa = 2$ , this approach showed significant drawbacks for values of  $\kappa \sim 50$  typical for practical type-II superconductors. Simulations were time consuming, unstable and mesh sensitive.

The goal of this paper is to build a COMSOL model that correctly describes the behaviour of superconductors with  $\kappa$  values around 50. This model is intended for later studies of pinning.

## 2. Governing equations

### 2.1 Time-dependent Ginzburg-Landau

In Ginzburg-Landau theory, a superconductor is described by a complex order parameter  $\psi$ , where  $|\psi|^2$  indicates the fraction of electrons condensed into a superfluid. The time evolution of the order parameter  $\psi$  in the presence of magnetic field  $\mathbf{B} = \nabla \times \mathbf{A}$  is given by the GL equations (in SI units):

$$\begin{aligned} \frac{\hbar^2}{2mD} \left( \frac{\partial}{\partial t} + i \frac{q}{\hbar} \phi \right) \psi = \\ - \frac{1}{2m} \left( \frac{\hbar}{i} \nabla - q\mathbf{A} \right)^2 \psi + \alpha\psi - \beta|\psi|^2\psi \quad (1) \\ \sigma \left( \frac{\partial \mathbf{A}}{\partial t} + \nabla \phi \right) = \frac{q\hbar}{2mi} (\psi^* \nabla \psi - \psi \nabla \psi^*) \\ - \frac{q^2}{m} |\psi|^2 \mathbf{A} - \frac{1}{\mu_0} \nabla \times \nabla \times \mathbf{A} \quad (2) \end{aligned}$$

Here,  $\hbar$  is Planck's constant divided by  $2\pi$ ,  $D$  is a phenomenological diffusion coefficient,  $q = 2e$  and  $2m$  are the charge and mass of a Cooper pair respectively. Furthermore,  $\alpha$  and  $\beta$  are phenomenological parameters,  $\sigma$  is the conductivity of the material in its normal state,  $\phi$  is the electric potential and  $\mu_0$  is the permeability of free space. The equations (1) and (2) can be derived from the minimization of the free energy  $F$  of a superconductor with respect to  $\psi$  and  $\mathbf{A}$  respectively.

Equation (2) assumes an externally applied uniform static field  $\mathbf{B}_a$  perpendicular to the plane

in which  $\mathbf{A} = [A_x, A_y]^T$  is solved for:  $\mathbf{B}_a = \hat{\mathbf{e}}_z B_z$ . Initially, a finite-sized superconductor is considered, subject to boundary conditions:

$$\begin{aligned} \left(\frac{\hbar}{i} \nabla \psi - q \mathbf{A} \psi\right) \cdot \mathbf{n} &= 0, \quad \text{on } \partial\Omega, \\ \nabla \times \mathbf{A} &= \mathbf{B}_a, \quad \text{on } \partial\Omega, \\ \left(\frac{\partial A}{\partial t} + \nabla \phi\right) \cdot \mathbf{n} &= 0, \quad \text{on } \partial\Omega, \end{aligned} \quad (3)$$

## 2.2 Material parameters $\lambda$ , $\xi$ and $\kappa$

Important material parameters that will be considered throughout this paper are the London penetration depth  $\lambda$ , the Ginzburg-Landau coherence length  $\xi = \hbar/\sqrt{2m\alpha}$ , and their ratio, the Ginzburg-Landau parameter  $\kappa = \lambda/\xi$ .

The London penetration depth  $\lambda$  characterises the distance to which a magnetic field penetrates into a superconductor. In the ideal one dimensional case  $\mathbf{B}$  is given by  $\mathbf{B}(d) = \mathbf{B}_a e^{-d/\lambda}$ , where  $d$  denotes the depth. Moreover, since a vortex has a self-sustaining normal conducting region inside a superconducting domain,  $\lambda$  is related to the width of the magnetic field peak that is associated with the vortex.

Furthermore, the Ginzburg-Landau coherence length  $\xi$  is related to the size of variations in  $|\psi|$  and is considered the ‘‘size’’ of the vortex core (i.e. the radius of the non-superconducting region). The ratio between the two:  $\kappa$ , denotes the size of the field peak with respect to the size of the vortex core. A high value is preferred since high  $\kappa$  materials superconduct in higher external fields.

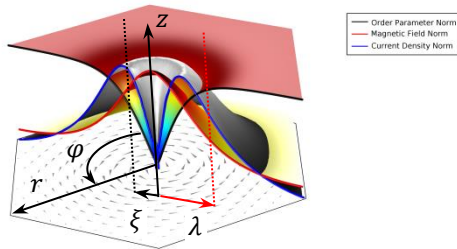


**Fig 1.** Illustration of a vortex in a type-II superconductor with  $\kappa = 2$ . The black, red and blue curves show  $|\psi|$ ,  $|\mathbf{B}|$ ,  $|\mathbf{J}|$  respectively, where  $\mathbf{J} = \nabla \times \mathbf{B}/\mu_0$ . The characteristic radii  $\lambda$  and  $\xi$  are indicated with the arrows and dotted lines.

## 2.2 Critical fields and field geometry

When  $\mathbf{B}_a = 0$ , the ground state of the superconductor is the Meissner state, with  $|\psi| = 1$  and  $\mathbf{B} = 0$  in the whole domain. As  $\mathbf{B}_a$  increases, at a certain point vortices become energetically favourable. This gives the first critical field:

$$B_{c1}(\kappa) = (\ln \kappa + \alpha(\kappa)) \Phi_0 / 4\pi\lambda^2 \quad (4)$$

with  $\Phi_0 = h/q$  the flux quantum and  $\alpha(\kappa)$  a non-trivial fit containing several parameters<sup>2</sup>. At  $\gg 1$   $\alpha(\kappa) = 0.49693$ .

As  $\mathbf{B}_a$  increases further, vortices penetrate the bulk of superconductor. Each vortex carries one flux quantum  $\Phi_0$ .

As long as the distance between the vortices is large compared to  $\lambda$ , the vortices show little interaction and are ‘‘isolated vortices’’. For  $\kappa \gg 1$  and  $r > \xi$ , (see fig. 1) the magnetic field shape and current density of these vortices are:

$$B_z(r/\lambda) = K_0(r/\lambda) \Phi_0 / 2\pi\lambda^2 \quad (5)$$

$$J_\varphi(r/\lambda) = K_1(r/\lambda) \Phi_0 / \mu_0 2\pi\lambda^3, \quad (6)$$

where  $B_z$  and  $J_\varphi$  are components of  $\mathbf{B}$  and  $\mathbf{J}$  (see fig. 1) and  $K_0, K_1$  are modified Bessel functions of the second kind.

When the distance between vortices becomes smaller, they form a flux-line lattice (FLL), also known as Abrikosov lattice. As  $\mathbf{B}_a$  increases, more vortices enter and the lattice becomes more compressed. At a certain point, the cores of vortices overlap and no superconducting path is left for a transport current. At this point, the second critical field is reached:

$$B_{c2} = \Phi_0 / 2\pi\xi^2 \quad (7)$$

and the size of the Abrikosov unit cell is:  $2\pi\xi^2$ .

## 2.3 Virial theorem and magnetisation

During the process described above, the average magnetic field inside the superconductor,  $\langle B \rangle = \int B_z dx dy / \int dx dy$ , lags behind the  $|\mathbf{B}_a|$ . The resulting magnetisation  $\mathbf{M}$  is:

$$\mathbf{M}(\mathbf{B}_a) = ((\mathbf{B}) - \mathbf{B}_a) / \mu_0 \quad (8)$$

As  $|\mathbf{B}_a|$  goes to  $B_{c2}$ ,  $|\mathbf{M}|$  goes to zero.

The dependence of  $\mathbf{M}$  on  $\mathbf{B}_a$  in ideal type-II superconductor was studied by Brandt and the resulting expression (for  $\kappa \geq 5$ ) is:

$$-m = \frac{1}{4\kappa^2} \ln \left( 1 + \frac{1-b}{b} f_2(b) \right),$$

$$f_2(b) = 0.357 + 2.890b - 1.581b^2 \quad (9)$$

with scaled magnetization:  $m = \mu_0 |\mathbf{M}| / B_{c2}$  and applied field  $b = |\mathbf{B}_a| / B_{c2}$ .

For a finite-sized superconductor, the applied field  $\mathbf{B}_a$  can be easily introduced in the boundary conditions. However, the ideal type-II superconductor is infinite and  $\mathbf{B}_a$  has no meaning. Instead,  $\mathbf{B}_a$  and  $\langle B \rangle$  are linked by the virial theorem<sup>2</sup>:

$$|\mathbf{B}_a| / \mu_0 = \langle |\psi|^2 - |\psi|^4 + 2B^2 \rangle / \langle 2B \rangle, \quad (10)$$

where  $\langle \dots \rangle$  denotes the spatial average over the domain.

## 2.4 Normalization and Gauge Invariance

The COMSOL implementation follows that of Alstrøm et al. This gives the following dimensionless Ginzburg-Landau equations:

$$\frac{\partial}{\partial t} \psi = - \left( \frac{i}{\kappa} \nabla + \mathbf{A} \right)^2 \psi + \psi - |\psi|^2 \psi \quad (11)$$

$$\sigma \frac{\partial}{\partial t} \mathbf{A} = \frac{1}{2i\kappa} (\psi^* \nabla \psi - \psi \nabla \psi^*)$$

$$-|\psi|^2 \mathbf{A} - \nabla \times \nabla \times \mathbf{A} \quad (12)$$

With the boundary conditions:

$$\nabla \psi \cdot \mathbf{n} = 0, \quad \text{on } \partial\Omega,$$

$$\nabla \times \mathbf{A} = \mathbf{B}_a, \quad \text{on } \partial\Omega,$$

$$\mathbf{A} \cdot \mathbf{n} = 0, \quad \text{on } \partial\Omega, \quad (13)$$

Critical fields:

$$B_{c1}(\kappa) = (\ln \kappa + \alpha(\kappa)) / 2\kappa \quad (14)$$

$$B_{c2}(\kappa) = \kappa \quad (15)$$

Or alternatively, with  $\Phi_0 = 2\pi/\kappa$  and  $\xi = 1/\kappa$ :

$$B_{c2} = \Phi_0 / 2\pi\xi^2 \quad (16)$$

Note that with the new definitions for  $\Phi_0$  and  $\xi$ , the expressions 16 and 7 are identical.

Furthermore, eqs. 5, 6, 8, 10 become:

$$B_z(r) = K_0(r) / \kappa \quad (17)$$

$$J_\varphi(r) = K_1(r) / \kappa \quad (18)$$

$$\mathbf{M}(\mathbf{B}_a) = \langle \mathbf{B} \rangle - \mathbf{B}_a \quad (19)$$

$$|\mathbf{B}_a| = \langle |\psi|^2 - |\psi|^4 + 2B^2 \rangle / \langle 2B \rangle \quad (20)$$

## 3. Method

### 3.1 Initial implementation

The initial implementation is identical to the one discussed in appendix A of Alstrøm et al<sup>1</sup>, with the exception that no additional auxiliary variable is introduced. Instead, the boundary condition  $\mathbf{A} \cdot \mathbf{n} = 0$  is directly applied, using a ‘‘pointwise constraint’’ (one of the available boundary conditions in COMSOL’s built-in PDE interfaces). The other boundary conditions, namely  $\nabla \psi \cdot \mathbf{n} = 0$  and  $\nabla \times \mathbf{A} = \mathbf{B}_a$ , are automatically applied by means of the default zero flux condition:  $-\mathbf{n} \cdot \mathbf{\Gamma} = 0$ . At  $\kappa = 2$ , this model reproduces the general vortex dynamics<sup>1</sup>.

However, as  $\kappa = \lambda/\xi$  increases, the situation changes. Since  $\xi$  is related to our model’s finest features (the  $|\psi| < 0.5|\psi|_{max}$  regions in the  $|\psi|$ -field, coloured blue in fig. 3), the mesh is defined in terms of  $\xi$ . Also, since  $\lambda$  is related to the size of the border effects and the distance between vortices (and therefore the size of the overall structure), the domain size is defined in terms of  $\lambda$ . As a consequence, higher  $\kappa$  requires larger domain with respect to the mesh size and therefore, a large number of degrees of freedom (DOF). As a result, at higher  $k$  it becomes unpractical to compute magnetisation curves with this approach.

### 3.2 Use of periodicity

In order to overcome this problem, we use a hexagonal geometry for a unit cell. The border effects are removed by replacing the external boundary conditions (as defined by Alstrøm et al<sup>1</sup>), by periodicity conditions:

$$-\mathbf{n}_{dst} \cdot \mathbf{\Gamma}_{dst} = \mathbf{n}_{src} \cdot \mathbf{\Gamma}_{src} \quad (21)$$

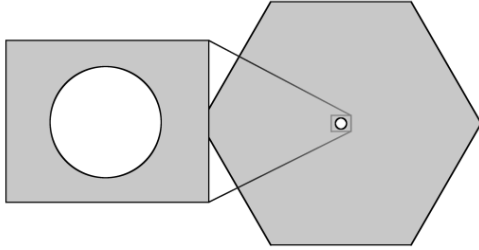


**Fig. 2** Hexagonal unit cell with periodicity on all sides and pinhole in the centre.

This implies the assumption of an infinite periodic vortex lattice (the Abrikosov lattice), with our domain being the unit cell.

### 3.3 Pinhole approach

Since external boundaries are absent in this model, a vortex enters from within the unit cell, through a pinhole of radius  $r \leq 0.01\xi$  placed at the cell centre, fig. 2. In this approach, the field near the external boundary condition (at the pinhole border) cannot be considered as the external field  $\mathbf{B}_a$  anymore. Given one flux quantum  $\Phi_0$  is in the cell, it is equal to the vortex central field  $\mathbf{B}_v$  that is related to  $\mathbf{B}_a$  through the virial theorem, eq. 20.

*Numerous benchmarks show validity of this approach.*

In particular, using multiple, connected unit cells (one of them containing a pinhole), the pinned vortex has been compared to free vortices (vortices that contain no pinhole). Excellent agreement has been found for  $|\psi|$  and  $\mathbf{B}$ , for large unit cells as well as for closely packed vortex lattices.

### 3.4 Magnetisation curve

In order to produce a magnetisation curve for  $0.01B_{c2} \leq |\mathbf{B}_a| \leq B_{c2}$ , the model includes an iterative process that reduces the unit cell size (and therefore the lattice constant) as  $\mathbf{B}_a$  increases so that the cell contains one flux quantum.

For each cell size, the vortex central field  $\mathbf{B}_v$  is ramped up by means of the pinhole border condition  $\nabla \times \mathbf{A} = \mathbf{B}_v$ , until one flux quantum is present. Using eqs. 19, 20, the resulting field  $\mathbf{B}$  the magnetisation  $\mathbf{M}$  are computed. This process

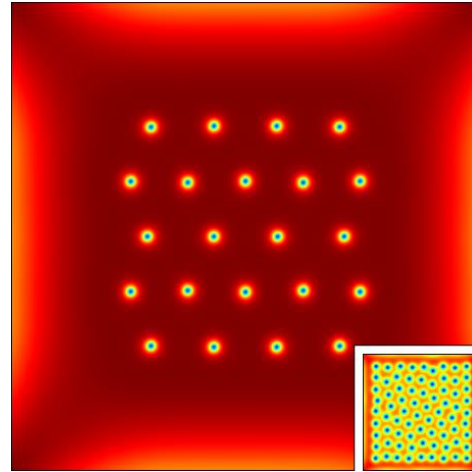


**Fig. 3** Computed  $|\psi|$ -field at  $\kappa = 2$  (small insert,  $16\lambda \times 16\lambda$ ) and  $\kappa = 50$  (large section,  $2.56\lambda \times 2.56\lambda$ ). As higher  $\kappa$  implies larger  $\lambda$ , border effects are more pronounced at higher  $\kappa$ . **Note:** the images are scaled in terms of  $\xi$ . In terms of  $\lambda$ , the large section is in fact, smaller. Both images are taken at  $\mathbf{B}_a = 1.4$ .

is repeated until  $|\mathbf{B}_a| = B_{c2}$  (at which the unit cell area is  $\Phi_0/B_{c2}$ ). At the end of the computation process, the collected values for  $\mathbf{M}$  and  $\mathbf{B}_a$  give a magnetisation curve. Taking proper normalisation into account (to compensate for coordinate transformations and use of different unit systems), these curves can be compared to eq. 9.

## 4. Results

### 4.1 Initial implementation

The initial implementation from Alstrøm et al<sup>1</sup> resulted in models that can reproduce general vortex dynamics, vortex lattices and an early version of a magnetisation curve.

Basic geometry shapes such as rectangles, squares and circles are tested (see also fig. 3), as well as periodicity conditions. As mentioned in section 3, the models give agree well at  $\kappa = 2$ , but for higher  $\kappa$  values the number of degrees of freedom is problematic.

### 4.2 Hexagonal unit cell

When using a hexagonal unit cell (fig. 2) with periodic conditions at the boundaries, a vortex is excited using a pinhole. For unit cells with radius  $R = 10^3\xi$  and above, the vortex can be seen as isolated, since the scaled magnetic field distribution around the pinhole is independent on the unit cell size.

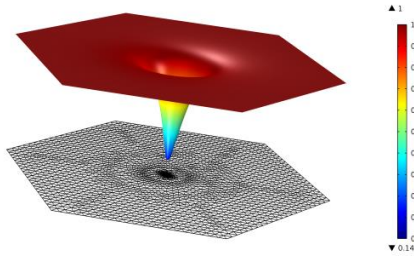


**Fig. 4** Computed  $|\psi|$ -field of an isolated vortex in a periodic hexagonal domain at  $\kappa = 50$ . For clarity, the size of the vortex relative to the unit cell has been greatly exaggerated. In practice, the unit cell radius  $\sim 10^3 \xi$ .

A comparison of the computed  $B_z(r)$  and  $J_\varphi(r)$  curves to the theory (see eqs. 17, 18, valid for  $\kappa \gg 1$  and  $r > \xi$ ), as well as to the graphs in figs. 4-6 from Brandt<sup>2</sup> show their reasonable agreement (see figs. 5a and b).

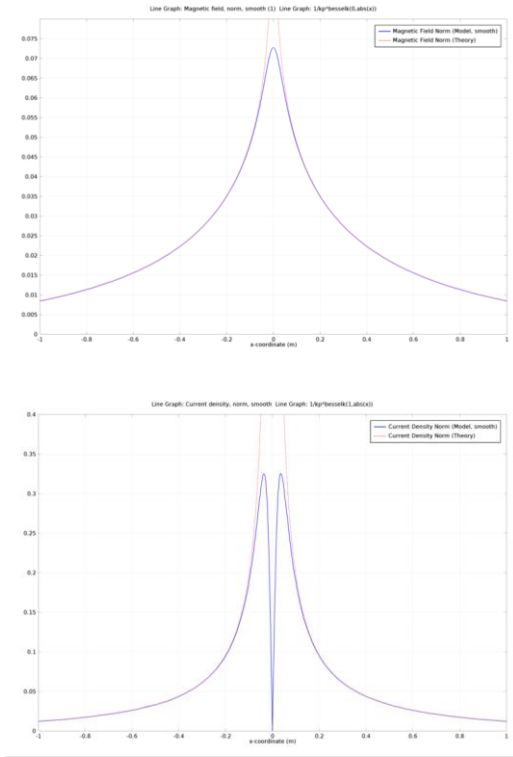


**Fig. 5a (top)** Comparison between the  $B_z = |\nabla \times \mathbf{A}|$  from the model (blue solid line) and the theory, eq. 17 (red dashed line). For  $r < \xi$ , the model converges to the vortex central field:  $B_z = B_v$ . In the centre, the model gives  $\partial B_z / \partial r = 0$  (as it should), while the theoretical curve loses validity and goes to infinity.

**Fig. 5b (bottom)** Comparison between the  $J_\varphi = |\nabla \times \mathbf{B}|$  from the model (blue solid line) and the theory, eq. 18 (red dashed line). For  $r < \xi$ , the model converges to zero (as it should), while the theoretical curve incorrectly goes to infinity.

### 4.3 Magnetisation

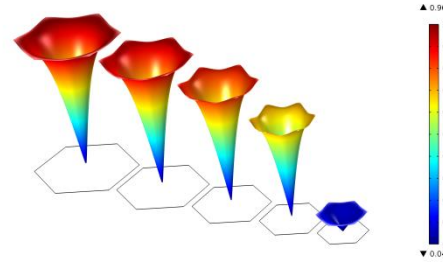


**Fig. 6** Evolution of the vortex  $|\psi|$ -field and of the unit cell size as  $B_a$  increases (from left to right): as  $|B_a|$  and  $|B_v|$  approach  $B_{c2}$ , the unit cell size approaches  $\Phi_0 / B_{c2}$ , and  $|\psi|$  goes to zero in the whole domain.

The computed magnetisation curve is compared to that of Brandt, eq. 9. The results are in perfect agreement, see example in fig. 7.

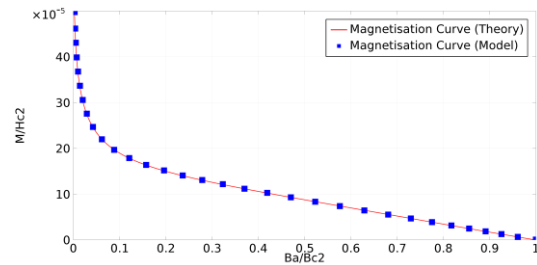


**Fig. 7** Magnetisation curve  $M(B_a)$  of ideal type II superconductor at  $k=50$  retrieved from<sup>2</sup> (red line) and computed using our model (blue dots).

### 5. Conclusions

- The COMSOL model of a superconductor from Alstrøm et al<sup>1</sup> shows correct behaviour at  $\kappa = 2$ . For  $\kappa = 50$ , the implementation becomes challenging because of the large number of degrees of freedom required.
- The problem can be solved by using periodicity conditions and a unit cell with variable size. Model using this approach, correctly reproduce vortex structure and  $B_{c2}$  for  $\kappa = 50$ .

- Computed magnetization of ideal type-II superconductor at  $\kappa = 50$  is in perfect agreement with the theory of Brandt.
- A new COMSOL model of type II superconductor is created and will be used to study effect of pinning in type-II superconductors at high values of  $\kappa$ .

## 6. References

1 Alstrøm

Tommy Sonne Alstrøm, Mads Peter Sørensen, Niels Falsig Pedersen, Søren Madsen - *Magnetic Flux Lines in Complex Geometry Type-II Superconductors Studied by the Time Dependent Ginzburg-Landau Equation* - Acta Appl. Math. **115**, 63 (2011).

2 Brandt

Ernst Helmut Brandt - *Properties of the ideal Ginzburg-Landau vortex lattice* - Phys. Rev. B **68**, 054506 (2003).

3 Berdiyrov

Golibjon Berdiyrov - *Vortex Structure and Critical Parameters in Superconducting Thin Films with Arrays of Pinning Centers* - (PhD thesis), University of Antwerpen (2007).

4 Pogosov

W. V. Pogosov, K. I. Kugel, A. L. Rakhmanov, E. H. Brandt - *Approximate Ginzburg-Landau solution for the regular flux-line lattice. Circular cell method* - Phys. Rev. B **64**, 064517 (2001).